



INDIAN INSTITUTE OF TECHNOLOGY BOMBAY

AE 593 - DUAL DEGREE PROJECT I

---

# **A Comparative Study of Turbulence Modelling for Smoothed Particle Hydrodynamics**

---

*Submitted By:*  
K T Prajwal Prathiksh  
180010027

*Supervisor:*  
Prof. Prabhu Ramachandran

*Report submitted in fulfillment of the requirements for Dual Degree Project I  
in the*

Department of Aerospace Engineering

October 14, 2022

DEPARTMENT OF AEROSPACE ENGINEERING

Indian Institute of Technology Bombay

## *Abstract*

### **A Comparative Study of Turbulence Modelling for Smoothed Particle Hydrodynamics**

by K T Prajwal Prathiksh

Hello, here is some text without a meaning. This text should show what a printed text will look like at this place. If you read this text, you will get no information. Really? Is there no information? Is there a difference between this text and some nonsense like “Huardest gefburn”? Kjift – not at all! A blind text like this gives you information about the selected font, how the letters are written and an impression of the look. This text should contain all letters of the alphabet and it should be written in of the original language. There is no need for special content, but the length of words should match the language.

**Keywords:** Fluid Mechanics, Turbulence Modelling, Smoothed Particle Hydrodynamics, Reynolds Averaging, Large Eddy Simulation, Lagrangian Averaging

# Contents

<b>Abstract</b>	<b>i</b>
<b>List of Figures</b>	<b>iii</b>
<b>List of Symbols</b>	<b>iv</b>
<b>1 Introduction</b>	<b>1</b>
1.1 Project Motivation . . . . .	1
1.2 Research Aims & Objectives . . . . .	1
1.3 Report Structure . . . . .	1
<b>2 Turbulence Modelling</b>	<b>2</b>
2.1 Viscosity-Based Models . . . . .	2
2.1.1 Eddy Viscosity Model . . . . .	2
2.1.2 Generalized Langevin Model . . . . .	3
2.2 mSPH . . . . .	5
2.3 Large Eddy Simulation-based Models . . . . .	6
2.3.1 Implicit Pressure Poisson-based Models . . . . .	6
2.3.2 Explicit Pressure Equation of State-based Solvers . . . . .	10
<b>Bibliography</b>	<b>13</b>

# List of Figures

2.1	Turbulent Poiseuille flow in a pipe ( $Re = 64e3$ ) modelled using the eddy viscosity model. Computed mean velocity profiles after ( $t = 1s$ ) (solid circles), against theory (solid line). Ref: (VIOLEAU, PICCON, and CHABARD 2002) . . . . .	3
2.2	Turbulent Poiseuille flow in a pipe ( $Re = 64e3$ ) modelled using the generalised Langevin model. Computed mean velocity profiles after ( $t = 1s$ ) (solid circles), against theory (solid line). Ref: (VIOLEAU, PICCON, and CHABARD 2002) . . . . .	4
2.3	Velocity vector plot at $t = 2$ (left) and $t = 30$ (right). $Re = \infty$ . Ref: (Adami, X. Y. Hu, and N. A. Adams 2012) . . . . .	6
2.4	Comparison of energy spectra $t = 10$ . $+$ and $\times$ denote standard SPH results with quintic spline and MLS interpolation; $\circ$ and $\square$ denote mSPH results with quintic spline and MLS interpolation. Ref: (Adami, X. Y. Hu, and N. A. Adams 2012) . . . . .	6
2.5	Dissipation rate at $Re = 400$ using DNS (solid line), Smagorinsky model (dashed line), standard SPH ( $+$ ) and mSPH ( $\circ$ ). Ref: (Adami, X. Y. Hu, and N. A. Adams 2012) . . . . .	7
2.6	Dissipation rate at $Re = 3000$ using DNS (solid line), Smagorinsky model (dashed line) and mSPH ( $\circ$ ). Ref: (Adami, X. Y. Hu, and N. A. Adams 2012) . . . . .	7
2.7	Time sequences of computational and experimental wave profiles near curtain wall (overtopping). Ref: (Gotoh, Shao, and Memita 2004) . . . .	11
2.8	Experimental and computational wave profiles by SPH and MPS model. Ref: (Shao and Gotoh 2005) . . . . .	12

# List of Symbols

Symbol	Description
$\mathbf{a}$	Vector Field
$\underline{\underline{\mathbf{A}}}$	Second-rank Tensor Field
$\hat{\mathbf{e}}_i$	$i^{th}$ Basis
$\frac{D()}{Dt}$	Lagrangian Derivative
$\langle \underline{\underline{\mathbf{A}}}, \underline{\underline{\mathbf{B}}} \rangle_F$	Frobenius Inner Product of $\underline{\underline{\mathbf{A}}}$ and $\underline{\underline{\mathbf{B}}}$
$\  \underline{\underline{\mathbf{A}}} \ _F$	Frobenius Norm of $\underline{\underline{\mathbf{A}}}$ ( $= \sqrt{\langle \underline{\underline{\mathbf{A}}}, \underline{\underline{\mathbf{A}}} \rangle_F}$ )
$\Delta()$	Component-wise Laplacian Operator
$i$	Reference Particle
$j$	Neighboring Particle
$(\dots)_i$	Property of $i^{th}$ SPH particle
$(\dots)_j$	Property of $j^{th}$ SPH particle
$(\dots)_{ij}$	$(\dots)_i - (\dots)_j$
$t$	Time
$\mathbf{r}$	Position
$\mathbf{v}$	Velocity
$m$	Mass
$P$	Pressure
$\rho$	Density
$\Delta x$	Inter Particle Spacing
$W_h$	SPH Interpolating Kernel
$h$	Kernel Smoothing Length
$W_{h,ij}$	$W(\mathbf{r}_{ij}, h)$
$\nabla_i W_{h,ij}$	$\nabla_i W(\mathbf{r}_{ij}, h)$

Table 1 continued from previous page

Symbol	Description
$\mathcal{V}_i$	Volume of $i^{th}$ SPH particle
$\mathbf{F}$	External Body Force
$\nu$	Kinematic Viscosity
$\eta$	Dynamic Viscosity ( $= \nu\rho$ )
$\varepsilon$	Machine Epsilon
$P_0$	Reference Pressure
$\rho_0$	Reference Density
$c_s$	Speed of Sound
$\gamma$	Exponent - Equation of State
$\nu_t$	Turbulent Eddy Viscosity
$\underline{\underline{\mathbf{S}}}$	Strain-Rate Tensor ( $= [1/2][\nabla\mathbf{v} + \nabla\mathbf{v}^T]$ )
$\epsilon$	Turbulent Dissipation Rate
$k$	Turbulent Kinetic Energy
$\underline{\underline{\boldsymbol{\tau}}}$	Stress Tensor
$C_s$	Smagorinsky Constant

## Chapter 1

# Introduction

Hello, here is some text without a meaning. This text should show what a printed text will look like at this place. If you read this text, you will get no information. Really? Is there no information? Is there a difference between this text and some nonsense like “Huardest gefburn”? Kjift – not at all! A blind text like this gives you information about the selected font, how the letters are written and an impression of the look. This text should contain all letters of the alphabet and it should be written in of the original language. There is no need for special content, but the length of words should match the language.

### 1.1 Project Motivation

### 1.2 Research Aims & Objectives

### 1.3 Report Structure

## Chapter 2

# Turbulence Modelling

### 2.1 Viscosity-Based Models

Violeau et al. (VIOLEAU, PICCON, and CHABARD 2002) were amongst the early pioneers who tried to incorporate a turbulence model in SPH. They came up with two techniques to tackle the problem of turbulence in a Lagrangian framework, which so far had been neglected till then in research, namely, the eddy viscosity model and a generalised Langevin model. For each of their techniques, they considered the following equation of state 2.1, continuity equation 2.2 and momentum equation 2.3, based on the work of (Monaghan 1992):

$$P_i = \frac{\rho_0 c_s^2}{\gamma} \left[ \left( \frac{\rho_i}{\rho_0} \right)^\gamma - 1 \right] \quad (2.1)$$

$$\frac{D\rho_i}{Dt} = \sum_j m_j \mathbf{v}_{ij} \cdot \nabla_i W_{h,ij} \quad (2.2)$$

$$\frac{D\mathbf{v}_i}{Dt} = \sum_j m_j \left( \frac{P_i}{\rho_i^2} + \frac{P_j}{\rho_j^2} + \Pi_{ij} \right) \nabla_i W_{h,ij} + \mathbf{F}_i \quad (2.3)$$

Where the viscous term is defined as:

$$\Pi_{ij} = -\frac{16\nu}{\rho_i + \rho_j} \frac{\mathbf{v}_{ij} \cdot \mathbf{r}_{ij}}{|\mathbf{r}_{ij}|^2 + \varepsilon^2} \quad (2.4)$$

#### 2.1.1 Eddy Viscosity Model

The eddy viscosity model was devised as a first-order closure model, which consisted of a relationship between the Reynolds stress tensor and the mean velocity gradients. Therefore, the momentum equation is similar to the momentum equation, except that the kinematic viscosity is replaced by the eddy viscosity ( $\nu_t$ ), and the velocities are Reynolds-averaged. In the SPH formalism, the diffusion term occurring is therefore defined as given in 2.5, with the eddy viscosity defined according to 2.6.

$$\tilde{\Pi}_{ij} = -8 \frac{\nu_{t,i} + \nu_{t,j}}{\rho_i + \rho_j} \frac{\langle \mathbf{v} \rangle_{ij} \cdot \mathbf{r}_{ij}}{|\mathbf{r}_{ij}|^2 + \varepsilon^2} \quad (2.5)$$

$$\nu_t = L_m^2 ||\underline{\underline{\mathbf{S}}}||_F = L_m^2 \sqrt{\langle \underline{\underline{\mathbf{S}}}, \underline{\underline{\mathbf{S}}} \rangle_F} \quad (2.6)$$

Where  $\langle \mathbf{v} \rangle$  is Reynolds-averaged velocity, and  $L_m$  refers to the mixing length scales. The SPH formulation for the mean velocity gradients are given in 2.7.



$$\nabla \langle \mathbf{v} \rangle_i = -\frac{1}{\rho_i} \sum_j m_j \langle \mathbf{v} \rangle_{ij} \otimes \nabla_i W_{h,ij} \quad (2.7)$$

On simulating Poiseuille flow for a high Reynolds number case, the authors could show that the velocity profile showed only a slight discrepancy with theory, with the expected log-law profile near the walls 2.1. This indicated that the model is appropriate for turbulent mixing problems or for cases involving spatially-varying viscosity while restricted to shear flows.

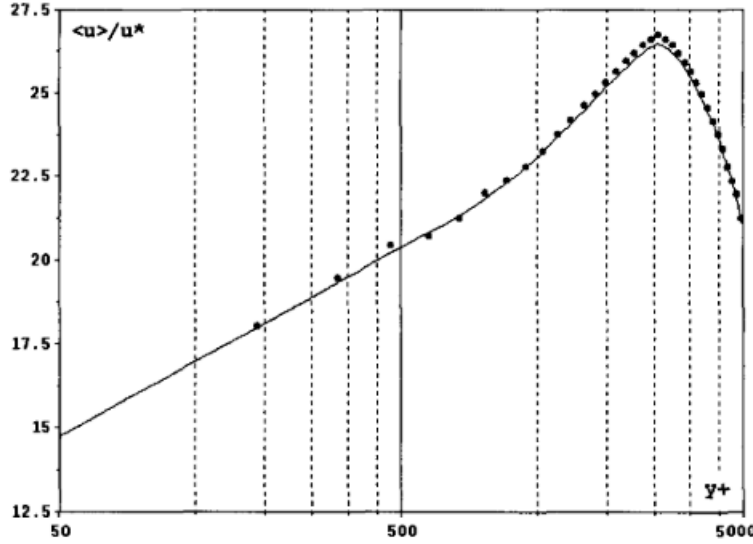


FIGURE 2.1: Turbulent Poiseuille flow in a pipe ( $Re = 64e3$ ) modelled using the eddy viscosity model. Computed mean velocity profiles after ( $t = 1s$ ) (solid circles), against theory (solid line). Ref: (VIOLEAU, PICCON, and CHABARD 2002)

### 2.1.2 Generalized Langevin Model

Violeau et al. also considered a stochastic approach, where the main idea is built on the concept of prescribing particle velocities as a random process, with properties fulfilling the theoretical turbulence hypotheses (Pope 1994). Hence, came about the Generalised Langevin model (GLM), where the particle acceleration is defined as:

$$d\mathbf{v} = -\frac{1}{\rho} \nabla \langle P \rangle + \underline{\underline{G}}(\mathbf{v} - \langle \mathbf{v} \rangle)dt + \sqrt{C_0 \epsilon} d\vec{\xi}, \quad (2.8)$$

Where  $\vec{\xi}$  is a random vector statistically non-correlated with velocities. The closure for this model was defined by specifying  $\underline{\underline{G}}$  as:

$$\underline{\underline{G}} = \frac{1}{2} C_1 \frac{\epsilon}{k} \mathbf{I} + C_2 \nabla \langle \mathbf{v} \rangle \quad (2.9)$$

Where ( $k$ ) is the turbulent kinetic energy, ( $\epsilon$ ) the dissipation rate, and ( $C_i$ ) being constants - ( $C_1 = 1.8, C_2 = 0.6$ ). By modelling turbulence as GLM in SPH, the

momentum equation derived was given by:

$$\frac{D\mathbf{v}_i}{Dt} = - \sum_j m_j \left( \frac{\langle P \rangle_i}{\rho_i^2} + \frac{\langle P \rangle_j}{\rho_j^2} \right) \nabla_i W_{h,ij} - \frac{1}{2} C_1 \frac{\epsilon_i}{k_i} \mathbf{v}'_i + C_2 \nabla \langle \mathbf{v} \rangle_i \cdot \mathbf{v}'_i + \sqrt{\frac{C_0 \epsilon_i}{\delta t}} \bar{\xi}_i \quad (2.10)$$

$$\langle \mathbf{v} \rangle = \sum_j \frac{m_j}{\rho_j} \mathbf{u}_j W_h(\mathbf{r}_j) \quad (2.11)$$

Where the fluctuations are defined as  $\mathbf{v}' = \mathbf{v} - \langle \mathbf{v} \rangle$ , and the local values of turbulent kinetic energy and dissipation rate are:

$$\epsilon_i = 2\nu_{t,i} + \|\underline{\mathbf{S}}_i\|_F^2 \quad (2.12)$$

$$k_i = \frac{\epsilon_i \nu_{t,i}}{C_\mu}, C_\mu = 0.009 \quad (2.13)$$

It is to be noted that the authors did not estimate the dissipation rate through the proper velocity gradients since the fluctuations of random velocities do not reproduce the small eddies. The same test case as mentioned in 2.1.1 was considered for the performance of GLM. The authors observed large fluctuations. They attributed the discrepancy to the mean operator being redefined as given by 2.11 instead of being a Reynolds average. In fact, by redefining the mean operator in such a fashion, they appeared to have constructed a rudimentary LES filter. As observed in 2.2, the fluctuations have an order of magnitude of  $k^{1/2}$ . However, as claimed by the authors, unlike the eddy viscosity model, the GLM method can be used for different flows instead of being restricted to only shear flows.

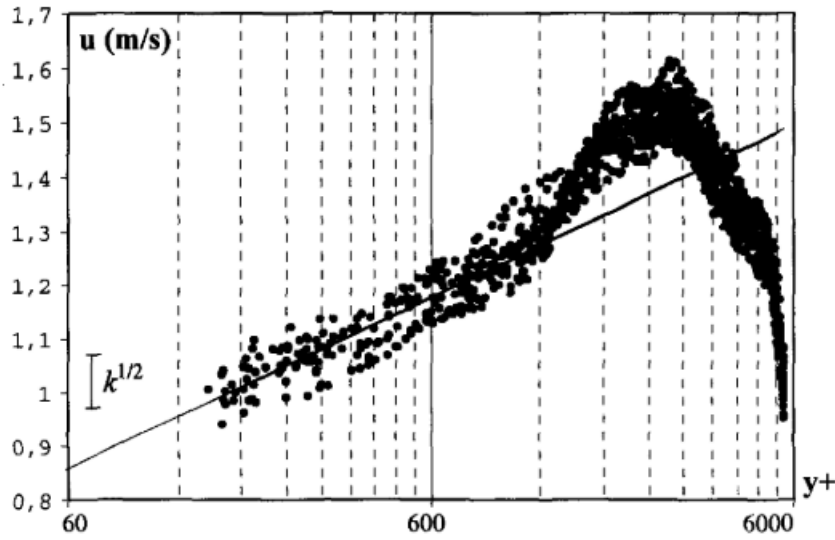


FIGURE 2.2: Turbulent Poiseuille flow in a pipe ( $Re = 64e3$ ) modelled using the generalised Langevin model. Computed mean velocity profiles after ( $t = 1s$ ) (solid circles), against theory (solid line).

Ref: (VIOLEAU, PICCON, and CHABARD 2002)

## 2.2 mSPH

Adami et al. (Adami, X. Y. Hu, and N. A. Adams 2012) devised a model built on their observation of SPH simulations, wherein the absence of viscosity in typical SPH formulations produced purely noisy particle motion. At finite viscosities, the method would over-predict dissipation. Hence to counter this, they essentially "modified" (hence the name: Modified SPH [mSPH]) the momentum equation and the equation of state to advect the particles in order to homogenise the particle distribution, in turn stabilising the numerical scheme. They were also able to reduce the artificial dissipation in transitional flows.

The authors considered summation density (2.15), which is a function of the volume of the respective SPH particle as given by 2.14, as opposed to evolving density through the continuity equation (Xiang Yu Hu and Nikolaus A Adams 2006). The modified equation of state as given by 2.16, is equivalent to the classical SPH equation-of-state with  $\gamma = 1$ .

$$\mathcal{V}_i = \frac{1}{\sum_j W_{h,ij}} \quad (2.14)$$

$$\rho_i = \frac{m_i}{\mathcal{V}_i} = m_i \sum_j W_{h,ij} \quad (2.15)$$

$$P_i = c_s^2(\rho_i - \rho_0) \quad (2.16)$$

The momentum equation, which provides the acceleration of the particle, is a function of just the gradient and viscous shear forces as given by 2.17. The corresponding SPH formulation was derived as given by 2.18, which built on the earlier work of Hu and Adams (X. Hu and Nikolaus A Adams 2007).

$$\frac{D\mathbf{v}}{Dt} = -\frac{1}{\rho}\nabla P + \nu\Delta(\mathbf{v}) + \mathbf{F} \quad (2.17)$$

$$\frac{D\mathbf{v}_i}{Dt} = -\frac{1}{m_i} \sum_j (\mathcal{V}_i^2 + \mathcal{V}_j^2) \frac{P_i\rho_j + P_j\rho_i}{\rho_i + \rho_j} \nabla_i W_{h,ij} - \frac{\eta}{m_i} \sum_j (\mathcal{V}_i^2 + \mathcal{V}_j^2) \frac{\mathbf{v}_{ij}}{|\mathbf{r}_{ij}|} \nabla_i W_{h,ij} + \mathbf{F}_i \quad (2.18)$$

This scheme takes advantage of the regularisation of the particle motion stemming from the additional background pressure ( $P_0 = \rho_0 c_s^2$ ). The additional force exerted by the background pressure counteracts non-homogeneous particle distributions, therein reducing numerical dissipation.

The authors estimated the energy spectra of the flow simulations in order to analyse the results of their test cases, using first and second-order moving-least-squares (MLS) method (GOSSLER 2001) and its subsequent Fourier transform (Frigo and Johnson 2005). Their first test case, the 2D variant of the Taylor-Green Vortex (TGV) problem, involved  $8 \times 8$  counter-rotating vortices, requiring  $64^2$  particles. They considered the viscosity to be zero. As seen in the time evolution of the

The time evolution of the velocity field is given in 2.3, where it can be observed that the 2D turbulence is characterised by merging and pairing of small vortices. The energy spectra given in 2.4 show that at low wave numbers, both interpolation schemes give the same results, but at high wave numbers, the results differ. The energy spectrum of the standard SPH has a linear slope of magnitude  $m = 1$  in a log-log scale equivalent to a purely noisy velocity field. Theoretically, however, 2D turbulence has an energy cascade with a slope of  $m = -3$  in the inertial range, which is reasonably predicted using mSPH.

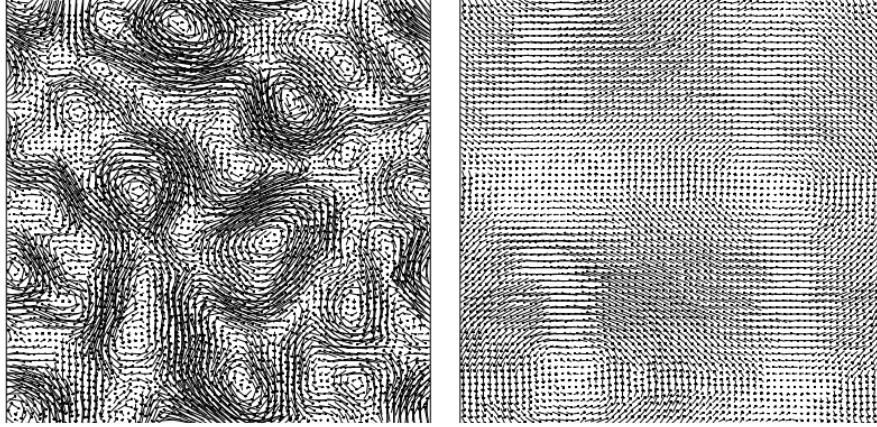


FIGURE 2.3: Velocity vector plot at  $t = 2$  (left) and  $t = 30$  (right).  
 $Re = \infty$ . Ref: (Adami, X. Y. Hu, and N. A. Adams 2012)

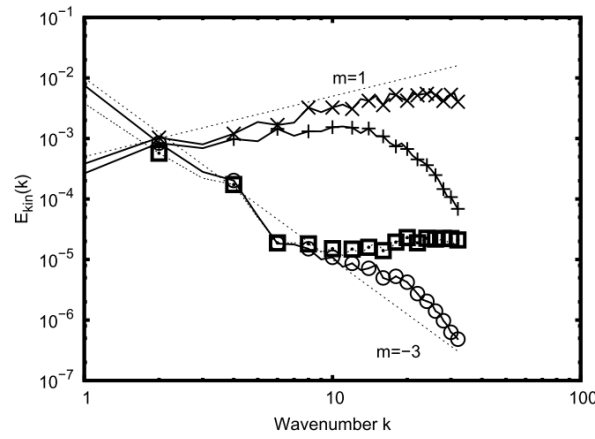


FIGURE 2.4: Comparison of energy spectra  $t = 10$ . + and  $\times$  denote standard SPH results with quintic spline and MLS interpolation;  $\circ$  and  $\square$  denote mSPH results with quintic spline and MLS interpolation. Ref: (Adami, X. Y. Hu, and N. A. Adams 2012)

The second test case employed by the authors was that of the 3D TGV problem requiring  $64^3$  particles for a wide range of Reynolds numbers. The dissipation rate of the flow simulations are shown in 2.5 and 2.6. It can be observed that the standard SPH is unable to simulate transitional flows due to excessive dissipation. In contrast, mSPH can reproduce the dissipation rate reasonably well. This implies that the corrected particle transport velocity is an analogous eddy-viscosity model on scales below the numerical resolution.

## 2.3 Large Eddy Simulation-based Models

### 2.3.1 Implicit Pressure Poisson-based Models

Gotoh et. al (Gotoh, Shao, and Memita 2004) were amongst the first to integrate Large Eddy Simulation techniques with SPH method. They derived this LES-SPH model, based on incompressible flow, so as to tackle the problem of reflection and transmission characteristics of regular waves by a partially immersed curtain-type

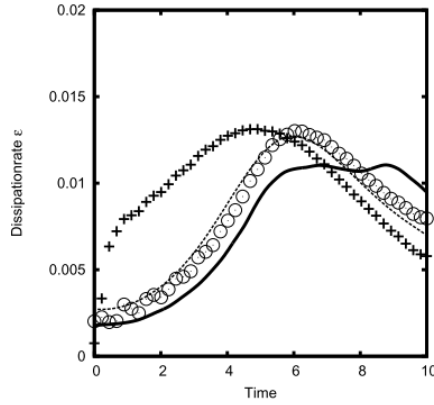


FIGURE 2.5: Dissipation rate at  $Re = 400$  using DNS (solid line), Smagorinsky model (dashed line), standard SPH (+) and mSPH (o). Ref: (Adami, X. Y. Hu, and N. A. Adams 2012)

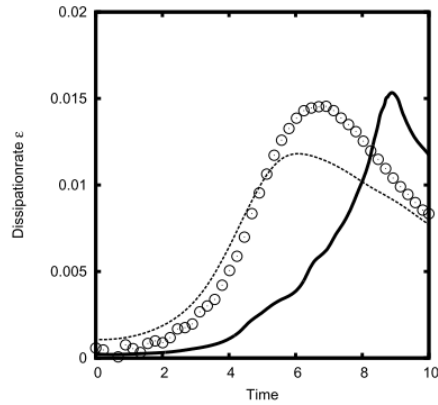


FIGURE 2.6: Dissipation rate at  $Re = 3000$  using DNS (solid line), Smagorinsky model (dashed line) and mSPH (o). Ref: (Adami, X. Y. Hu, and N. A. Adams 2012)

breakwater. In order to compare the dissipation efficiencies, they considered the non-overtopping and overtopping cases of the problem.

The governing equations of the system was described as given by the continuity equation in 2.19 and momentum equation in 2.17.

$$\frac{1}{\rho} \frac{D\rho}{Dt} + \nabla \cdot \mathbf{v} = 0 \quad (2.19)$$

The LES mass and momentum conservation equations for the flow was derived by filtering the respective equations using a spatial filter  $\overline{(\dots)}$  to obtain their filtered counter-parts as given by 2.20 and 2.21 respectively.

$$\frac{1}{\rho} \frac{D\rho}{Dt} + \nabla \cdot \bar{\mathbf{v}} = 0 \quad (2.20)$$

$$\frac{D\bar{\mathbf{v}}}{Dt} = -\frac{1}{\rho} \nabla \bar{P} + \nu \Delta(\bar{\mathbf{v}}) + \frac{1}{\rho} \nabla \cdot \underline{\underline{\tau}} + \mathbf{F} \quad (2.21)$$

$$\frac{1}{\rho} \underline{\underline{\tau}} = \bar{\mathbf{v}} \otimes \bar{\mathbf{v}} - \overline{\mathbf{v} \otimes \mathbf{v}} \quad (2.22)$$

The stress tensor defined in 2.22 is closed using the Boussinesq's Hypothesis as defined in 2.23.

$$\frac{1}{\rho} \underline{\underline{\tau}} = 2\nu_t \underline{\underline{S}} - \frac{2}{3} k \underline{\underline{I}} \quad (2.23)$$

The turbulent eddy viscosity is estimated using a modified Smagorinsky model as given in 2.24. This allows wall effects to be incorporated in the model, which was required by the authors in order to tackle the problem they were working on.

$$\nu_t = \min(C_s \Delta x, \kappa d_{wall})^2 \sqrt{2 \langle \underline{\underline{S}}, \underline{\underline{S}} \rangle_F} \quad (2.24)$$

$$C_s = 0.1, \kappa = 0.4 \quad (2.25)$$

Where,  $(C_s)$  is the Smagorinsky constant,  $(\kappa)$  is the von Karman constant and  $d_{wall}$  is the normal distance of particle to the closest wall. The first term in 2.24 dominates the flow far away from the solid wall, thereby recovering the standard Smagorinsky model. However, for flow close to the wall, the second term dominates and hence the eddy viscosity is a function of the particle distance to the wall. This overcomes the disadvantage of the standard Smagorinsky being over-dissipative inside the laminar layer.

In order to system of equations, and evolve them in time, the authors employed the Predictive-Corrective time integrator, similar to the two-step projection method of Chorin (Chorin 1968). The prediction stage is outlined by 2.26 - 2.28.

$$\Delta \mathbf{v}_* = \left( \nu \Delta(\bar{\mathbf{v}}) + \frac{1}{\rho} \nabla \cdot \underline{\underline{\tau}} + \mathbf{F} \right) \Delta t \quad (2.26)$$

$$\mathbf{v}_* = \mathbf{v}_t + \Delta \mathbf{v}_* \quad (2.27)$$

$$\mathbf{r}_* = \mathbf{r}_t + \mathbf{v}_* \Delta t \quad (2.28)$$

The correction stage is outlined by 2.29 - 2.32.  $(\bar{P})$  which is required to update the  $(\mathbf{v}_{t+1})$  term is calculated implicitly from 2.30, which is based on the filtered continuity equation given by 2.20 and assuming incompressibility  $\frac{D\rho}{Dt} = 0$ .

$$\Delta \mathbf{v}_{**} = -\frac{1}{\rho} \nabla \bar{P}_{t+1} \Delta t \quad (2.29)$$

$$\nabla \cdot \left( \frac{1}{\rho_*} \nabla \bar{P}_{t+1} \right) = \frac{\rho_0 - \rho_*}{\rho_0 \Delta t^2} \quad (2.30)$$

$$\mathbf{v}_{t+1} = \mathbf{v}_* + \Delta \mathbf{v} \quad (2.31)$$

$$\mathbf{r}_{t+1} = \mathbf{r}_t + (\mathbf{v}_t + \mathbf{v}_{t+1}) \frac{\Delta t}{2} \quad (2.32)$$

In order to solve the system of equations given by 2.26 - 2.32 in an SPH setting, the authors presented the following SPH formulation for the flow property. *Note:* The over-line  $(\overline{\dots})$  convention used to denote filtered flow properties will be dropped in this sub-section, unless stated otherwise.

The fluid density is given using a simple summation density 2.33.

$$\rho_i = \sum_j m_j W_{h,ij} \quad (2.33)$$



The pressure gradient term is defined in 2.34 in a symmetric form.

$$\left(\frac{1}{\rho}\nabla P\right)_i = \sum_j m_j \left(\frac{P_i}{\rho_i^2} + \frac{P_j}{\rho_j^2}\right) \nabla_i W_{h,ij} \quad (2.34)$$

The divergence of  $\mathbf{v}$  is also defined symmetrically as given by 2.35.

$$\nabla \cdot \mathbf{v}_i = \rho_i \sum_j m_j \left(\frac{\mathbf{v}_i}{\rho_i^2} + \frac{\mathbf{v}_j}{\rho_j^2}\right) \cdot \nabla_i W_{h,ij} \quad (2.35)$$

The pressure Laplacian, defined in 2.36, is formulated as a hybrid of a standard SPH first derivative with a finite difference approximation for the first derivative, so as to aid particle pressure stability (Cummins and Rudman 1999).

$$\nabla \cdot \left(\frac{1}{\rho}\nabla P\right)_i = \sum_j m_j \frac{8}{(\rho_i + \rho_j)^2} \frac{P_{ij} \mathbf{r}_{ij} \cdot \nabla_i W_{h,ij}}{|\mathbf{r}_{ij}|^2} \quad (2.36)$$

The divergence of the stress tensor is defined in 2.37.

$$\left(\frac{1}{\rho}\nabla \cdot \underline{\underline{\tau}}\right)_i = \sum_j m_j \left(\frac{1}{\rho_i^2} \underline{\underline{\tau}}_i + \frac{1}{\rho_j^2} \underline{\underline{\tau}}_j\right) \cdot \nabla_i W_{h,ij} \quad (2.37)$$

Finally the laminar stress term, consisting of the velocity Laplacian term, is defined as given by 2.38.

$$(v\Delta(\mathbf{v}))_i = \sum_j m_j \frac{4(\eta_i + \eta_j)}{(\rho_i + \rho_j)^2} \frac{\mathbf{v}_{ij} \mathbf{r}_{ij} \cdot \nabla_i W_{h,ij}}{|\mathbf{r}_{ij}|^2} \quad (2.38)$$

The authors used this SPH-LES model to investigate the wave interaction with partially immersed breakwater, and compared the results with experimentally obtained values of a similar setup. Their computational domain was 2D populated by  $\approx 12e3$  particles.

As observed in the comparative plots given in 2.7, the model proves to be accurate in tracking free-surfaces of large deformation without numerical diffusion. The authors also observed the capability of the model in simulating turbulence and eddy vortices realistically near the curtain wall. However, the authors also conclude that a more refined turbulence model will be required for further accuracy in predicting flow involving wave interactions.

Building on the work mentioned above, Shao and Gotoh (Shao and Gotoh 2005), performed a comparative study of SPH and Moving Particle Semi-Implicit (MPS) method coupled with a LES model. They also validated these models against experimental data.

The filtered conservation equations which the authors considered were the same as given by 2.20 - 2.23. However, they incorporated the standard Smagorinsky model (Smagorinsky 1963) given by 2.39 as opposed to the modified model 2.24.

$$v_t = (C_s \Delta x)^2 \quad (2.39)$$

The authors consider the same predictive-corrective scheme to evolve their system as detailed in 2.26 - 2.32. Similarly, they follow the same SPH formulation outlined in 2.33 - 2.38. They do however, slightly modify the pressure and velocity

Laplacian terms as given in 2.40 and 2.41 respectively.

$$(\nabla^2 P)_i = \sum_j m_j \frac{4}{\rho_i + \rho_j} \frac{P_{ij} \mathbf{r}_{ij} \cdot \nabla_i W_{h,ij}}{|\mathbf{r}_{ij}|^2} \quad (2.40)$$

$$(\nu \Delta(\mathbf{v}))_i = \sum_j m_j \frac{2(\nu_i + \nu_j)}{\rho_i + \rho_j} \frac{\mathbf{v}_{ij} \mathbf{r}_{ij} \cdot \nabla_i W_{h,ij}}{|\mathbf{r}_{ij}|^2} \quad (2.41)$$

The authors validated this SPH-LES Model using experimental data from the experimental data corresponding to a solitary wave breaking on the beach (Synolakis 1986). Their computational domain was 2D and consisted of  $\approx 18e3$  particles. From the computed wave profiles shown in 2.8, it can be visually observed that there is reasonable agreement between the experimental and computation data. This again verifies the accuracy of the model in tracking free surfaces with less or no numerical diffusion. Furthermore, by performing a convergence study of the SPH-LES model using the dam-break problem, the authors were able to show that the spatial and temporal accuracy of the scheme is  $O(\Delta t + \Delta x^{1.25})$ .

### 2.3.2 Explicit Pressure Equation of State-based Solvers

Weakly compressible solvers



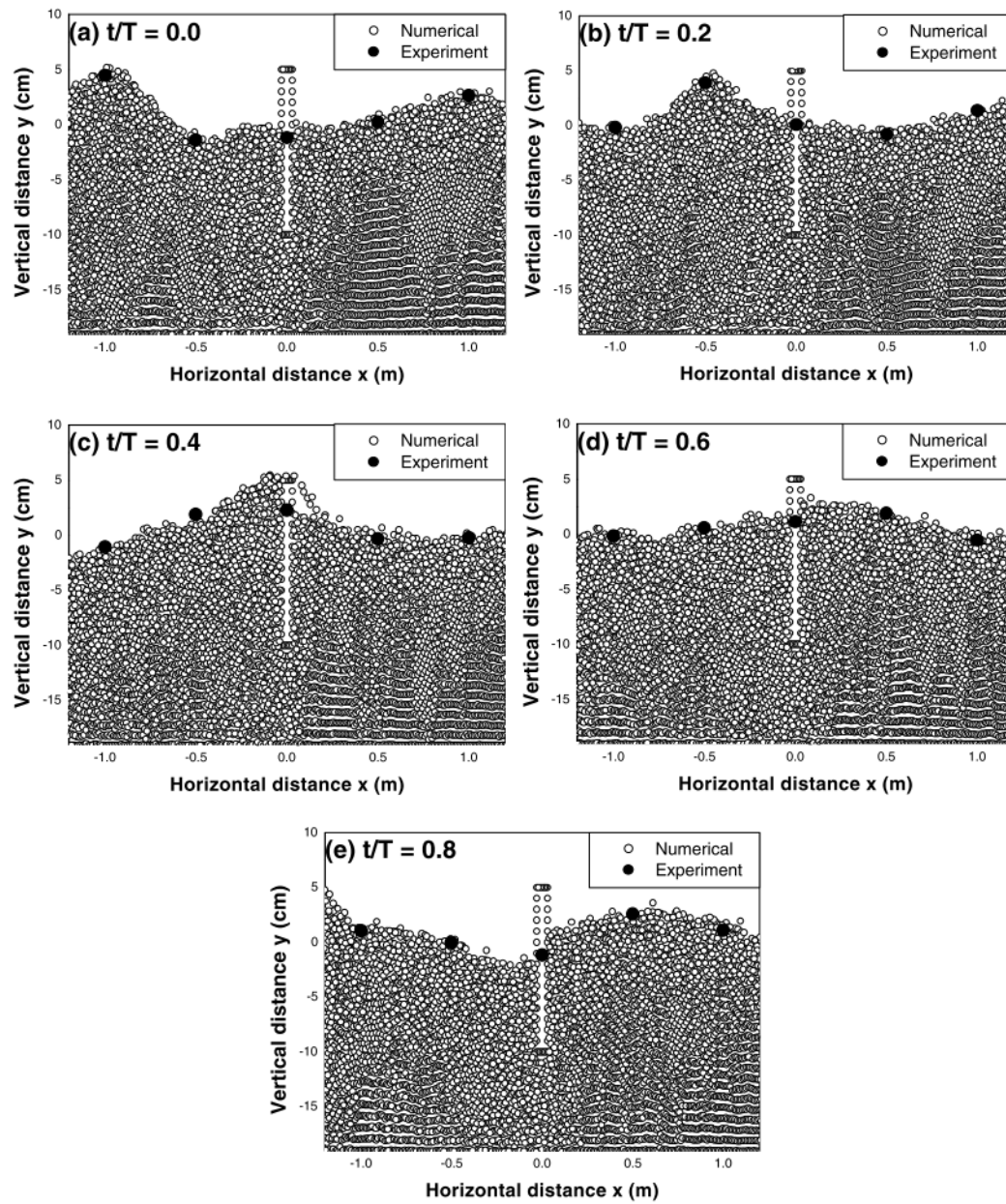


FIGURE 2.7: Time sequences of computational and experimental wave profiles near curtain wall (overtopping). Ref: (Gotoh, Shao, and Memita 2004)

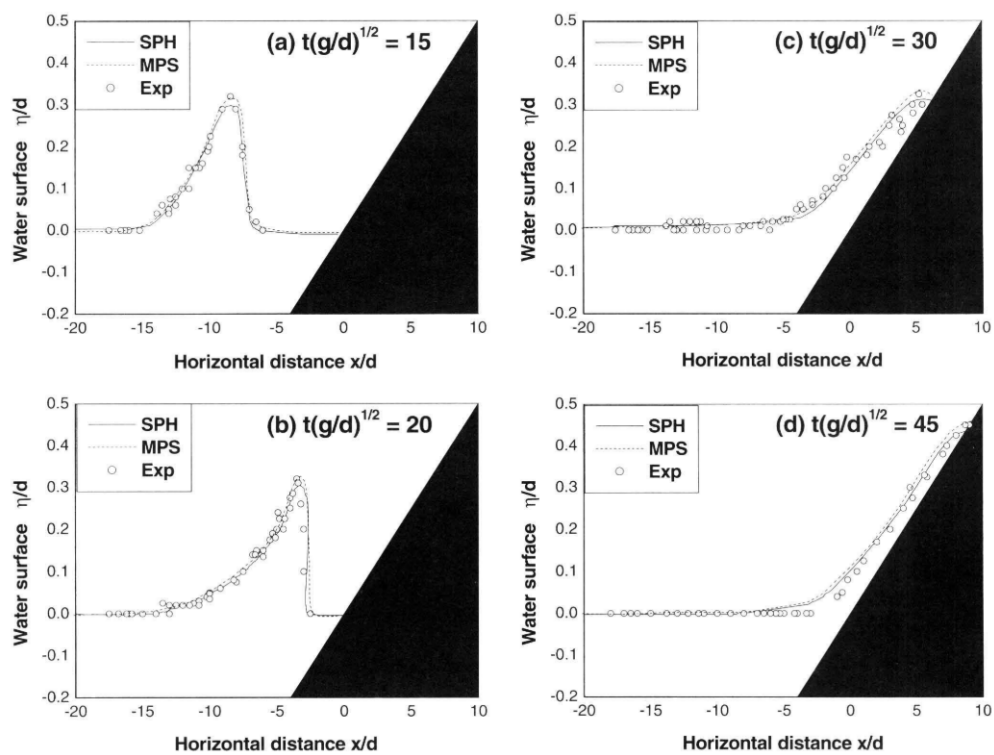


FIGURE 2.8: Experimental and computational wave profiles by SPH and MPS model. Ref: (Shao and Gotoh 2005)

# Bibliography

- Adami, S., X. Y. Hu, and N. A. Adams (2012). *Simulating three-dimensional turbulence with SPH*. Lehrstuhl für Aerodynamik.
- Chorin, Alexandre Joel (1968). "Numerical solution of the Navier-Stokes equations". In: *Mathematics of computation* 22.104, pp. 745–762.
- Cummins, Sharen J and Murray Rudman (1999). "An SPH projection method". In: *Journal of computational physics* 152.2, pp. 584–607.
- Frigo, Matteo and Steven G Johnson (2005). "The design and implementation of FFTW3". In: *Proceedings of the IEEE* 93.2, pp. 216–231.
- GOSSLER, ALBERT A (2001). *Moving Least-Squares: a numerical differentiation method for irregularly spaced calculation points*. Tech. rep. Sandia National Lab.(SNL-NM), Albuquerque, NM (United States); Sandia ...
- Gotoh, Hitoshi, Songdong Shao, and Tetsu Memita (2004). "SPH-LES model for numerical investigation of wave interaction with partially immersed breakwater". In: *Coastal Engineering Journal* 46 (1), pp. 39–63. ISSN: 17936292. DOI: [10.1142/S0578563404000872](https://doi.org/10.1142/S0578563404000872).
- Hu, Xiang Yu and Nikolaus A Adams (2006). "A multi-phase SPH method for macroscopic and mesoscopic flows". In: *Journal of Computational Physics* 213.2, pp. 844–861.
- Hu, XY and Nikolaus A Adams (2007). "An incompressible multi-phase SPH method". In: *Journal of computational physics* 227.1, pp. 264–278.
- Monaghan, J. J. (Sept. 1992). "Smoothed particle hydrodynamics". In: *Annual Review of Astronomy and Astrophysics* 30.1, pp. 543–574. ISSN: 00664146. DOI: [10.1146/annurev.aa.30.090192.002551](https://doi.org/10.1146/annurev.aa.30.090192.002551). URL: <http://adsabs.harvard.edu/full/1992ARA%7B%5C%7DA..30..543M%20http://www.annualreviews.org/doi/10.1146/annurev.aa.30.090192.002551>.
- Pope, SB (1994). "LAGRANGIAN PDF METHODS FOR TURBULENT FLOWS". In: *Annu. Rev. Fluid Mech* 23, p. 63.
- Shao, Songdong and Hitoshi Gotoh (May 2005). "Turbulence particle models for tracking free surfaces". In: *Journal of Hydraulic Research* 43.3, pp. 276–289. ISSN: 0022-1686. DOI: [10.1080/00221680509500122](https://doi.org/10.1080/00221680509500122). URL: <https://www.tandfonline.com/doi/full/10.1080/00221680509500122>.
- Smagorinsky, Joseph (1963). "General circulation experiments with the primitive equations: I. The basic experiment". In: *Monthly weather review* 91.3, pp. 99–164.
- Synolakis, Constantine Emmanuel (1986). "The runup of long waves". PhD thesis. California Institute of Technology.
- VIOLEAU, D., S. PICCON, and J.-P. CHABARD (July 2002). "TWO ATTEMPTS OF TURBULENCE MODELLING IN SMOOTHED PARTICLE HYDRODYNAMICS". In: vol. 1. WORLD SCIENTIFIC, pp. 339–346. ISBN: 978-981-02-4931-1. DOI: [10.1142/9789812777591\\_0041](https://doi.org/10.1142/9789812777591_0041). URL: [http://guest.cnki.net/grid2008/brief/detailj.aspx?filename=DZDQ200901001251&dbname=CPFD2010%20http://www.worldscientific.com/doi/abs/10.1142/9789812777591\\_0041](http://guest.cnki.net/grid2008/brief/detailj.aspx?filename=DZDQ200901001251&dbname=CPFD2010%20http://www.worldscientific.com/doi/abs/10.1142/9789812777591_0041).